

<https://helda.helsinki.fi>

Atmospheric Fate of Monoethanolamine : Enhancing New Particle Formation of Sulfuric Acid as an Important Removal Process

Xie, Hong-Bin

2017-08-01

Xie , H-B , Elm , J , Halonen , R , Myllys , N , Kurten , T , Kulmala , M & Vehkamäki , H 2017 , ' Atmospheric Fate of Monoethanolamine : Enhancing New Particle Formation of Sulfuric Acid as an Important Removal Process ' , Environmental Science & Technology , vol. 51 , no. 15 , pp. 8422-8431 . <https://doi.org/10.1021/acs.est.7b02294>

<http://hdl.handle.net/10138/299835>

<https://doi.org/10.1021/acs.est.7b02294>

acceptedVersion

Downloaded from Helda, University of Helsinki institutional repository.

This is an electronic reprint of the original article.

This reprint may differ from the original in pagination and typographic detail.

Please cite the original version.

The Atmospheric Fate of Monoethanolamine: Enhancing New-particle Formation of Sulfuric Acid as an Important Removal Process

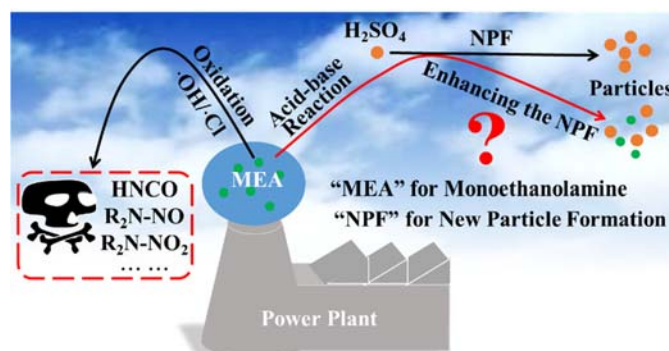
Hong-Bin Xie^{†‡}, Jonas Elm[‡], Roope Halonen[‡], Nanna Myllys[‡], Theo Kurtén[§], Markku Kulmala[‡] and Hanna Vehkamäki[‡]

[†]Key Laboratory of Industrial Ecology and Environmental Engineering (Ministry of Education), School of Environmental Science and Technology, Dalian University of Technology, Dalian 116024, China

[‡]Department of Physics, University of Helsinki, P. O. Box 64, FIN-00014 Helsinki, Finland

[§]Department of Chemistry, University of Helsinki, P. O. Box 55, FIN-00014 Helsinki, Finland

Table of Contents (TOC)



ABSTRACT. Monoethanolamine (MEA), a potential atmospheric pollutant from capture unit of a leading CO₂ capture technology, could be removed by participating H₂SO₄-based new particle formation (NPF) as simple amines. Here we evaluated the enhancing potential of MEA on H₂SO₄-based NPF by examining the formation of molecular clusters of MEA and H₂SO₄ using a combined quantum chemistry

calculations and kinetics modeling. The results indicate that MEA at ppt-level can enhance H_2SO_4 -based NPF. The enhancing potential of MEA is $<$ dimethylamine (DMA), one of the strongest enhancing agents, and \gg methylamine (MA), in contrast to the order suggested solely by their basicity ($\text{MEA} < \text{MA} < \text{DMA}$). The unexpectedly high enhancing potential is attributed to the role of $-\text{OH}$ of MEA in increasing cluster binding free energies by acting as both hydrogen bond donor and acceptor. After the initial formation of one H_2SO_4 and one MEA cluster, the cluster growth mainly proceeds by first adding one H_2SO_4 , and then one MEA, which differs from growth pathways in H_2SO_4 -DMA and H_2SO_4 -MA systems. Importantly, the effective removal rate of MEA due to participation in NPF is comparable to that of oxidation by hydroxyl radicals at 278.15 K, indicating NPF as an important sink for MEA.

INTRODUCTION

Monoethanolamine (MEA, $\text{NH}_2\text{CH}_2\text{CH}_2\text{OH}$) is a benchmark and widely utilized solvent in amine-based postcombustion CO_2 capture (PCC) technology.¹⁻⁹ Given the possible large-scale implementation of amine-based PCC, it is likely that there will be relatively significant emissions of MEA or other alkanolamines to the atmosphere from PCC units due to their relatively high vapor pressure.¹⁰ It has been estimated that a CO_2 capture plant which removes 1 million tons CO_2 per year from flue gas using MEA as solvent could potentially emit 80 tons MEA into the atmosphere.^{11,12} Therefore, in recent years concern about the atmospheric fate of the representative amine MEA has been increasing,^{6,13-22} as MEA could potentially form an environmental risk.^{11,12,17}

Several studies have addressed the removal of MEA by atmospheric oxidation.^{6,13-22} The oxidation by hydroxyl radicals ($\cdot\text{OH}$) has been considered to be its main degradation pathway, followed by chlorine radicals ($\cdot\text{Cl}$) at daytime.¹³ The nitrate radical may play a significant role in MEA oxidation at night, though very little is known about this pathway. The reaction rate constants of MEA with $\cdot\text{OH}$ and $\cdot\text{Cl}$ are in the order of 10^{-11} and $10^{-10} \text{ cm}^3 \text{ molecule}^{-1} \text{ s}^{-1}$, respectively, translating to 2.6-3.6 hours atmospheric lifetime.^{6,13,14,18,19} More importantly, atmospheric oxidation of MEA by $\cdot\text{OH}$ and $\cdot\text{Cl}$ can produce potentially hazardous compounds (such as isocyanic acid, HNCO, nitramine and nitrosamine),^{6,13,19} which can increase the environmental risk of MEA emission. Besides oxidation, acid-base reaction could be another important sink for MEA. However, the atmospheric fate related to the basicity of MEA has received little attention until now.

Atmospheric aerosol particles, at least 50% of which originates from new-particle formation (NPF), are known to affect human health and remain one of the leading uncertainties in global climate modeling and prediction.²³⁻²⁷ Many studies have shown that atmospheric bases such as ammonia and amines stabilize sulfuric acid clusters in the lower troposphere via acid-base reactions, and therefore enhance H_2SO_4 -based NPF rates.^{25,28-42} Compared to ammonia, amines, including monomethylamine (MA), dimethylamine (DMA) and trimethylamine (TMA), can bind much more strongly to sulfuric acid molecules^{29,40-43} and thus can efficiently enhance clustering sulfuric acid.⁴³ Recent work by Almeida et al. performed at the CLOUD chamber at CERN

shows that 5 ppt of dimethylamine can enhance NPF rates more than 10000 times compared with the case of 5 ppt ammonia, and is sufficient to produce particle formation rates of the same order of magnitude as observed in the atmosphere.²⁵ Besides ammonia, MA, DMA and TMA, atmospheric diamines were recently found to efficiently enhance NPF.^{44,45}

In a similar fashion to simple alkylamines, MEA can potentially influence NPF via acid-base reactions and therefore participating in NPF could be another atmospheric sink of MEA. A recent study highlighted the possible role of emitted amines from CO₂ capture unit of PCC in enhancing NPF.²⁵ The basicity of MEA is higher than that of ammonia and lower than that of methylamine and dimethylamine (pK_b values of MEA 4.50, MA 3.36, DMA 3.29, ammonia 5.7).⁴⁶ If judged solely by the basicity, MEA should have a higher enhancing effect on H₂SO₄-based NPF than NH₃, and lower effect than MA and DMA when atmospheric concentration of MEA is assumed to be similar to that of NH₃, MA and DMA. From the point of molecular structure, MEA has additional -OH compared to ammonia, MA and DMA. When forming clusters between MEA and H₂SO₄, the -OH group in MEA can form additional hydrogen bonds (H-bonds), which increase the binding energy of MEA with H₂SO₄. The conflicting effects of one favorable (more H-bonds) and one unfavorable factor (decreased basicity compared with methylamine and dimethylamine) could make it difficult to estimate how strong the enhancing effect of MEA will be. No previous studies have considered the potential role of alkanolamines in NPF involving H₂SO₄. An additional -OH in the

amine may lead to a different NPF pathway and rate compared to the ammonia/MA/DMA-H₂SO₄ systems. Therefore, to obtain a complete view of the atmospheric fate of MEA and extend the current knowledge of NPF involving amines and H₂SO₄, information about the potential of MEA to participate in atmospheric NPF is crucial.

In this study, we investigate the initial step of atmospheric H₂SO₄-based NPF by examining the formation of molecular clusters of MEA and sulfuric acid using a combination of quantum chemistry calculations and kinetics modeling employing the Atmospheric Cluster Dynamics Code^{47,48} (ACDC). Via systematic conformational searches, we have obtained minimum free energy structures of clusters of composition (MEA)_m(SA)_n ($m=0-4$ and $n=1-4$, “SA” represents H₂SO₄). The corresponding thermodynamic data and previously reported results for pure sulfuric acid (SA)₁₋₄ clusters⁴⁹ are used in ACDC to obtain cluster formation pathways and kinetics in the MEA-H₂SO₄ system. In addition, the effect of hydration on the cluster formation kinetics of MEA and H₂SO₄ is considered.

COMPUTATIONAL DETAILS

Electronic Structure Calculations. The most critical parameters in identifying cluster formation pathways and kinetics are the cluster formation free energies. Both minimum free energy structures of clusters (MEA)_m(SA)_n ($m=0-4$ and $n=0-4$) and computational method will determine the reliability of calculated cluster formation free energies. Here, a global minimum sampling technique (Figure 1), which has previously been applied

104 to study atmospheric cluster formation,^{45,50,51} was used to search for the global minima
105 of clusters (MEA)_m(SA)_n($m=1-4$ and $n=0-4$). The pure (SA)₁₋₄ clusters were taken from
106 the work of Ortega et al.⁴⁹ In Figure 1, all optimizations, frequency or single point
107 energy calculations with density functional theory and semiempirical PM6 level have
108 been performed in GAUSSIAN 09.⁵² The ω B97X-D functional was selected as the core
109 optimization and frequency calculation method in Figure 1, since it has shown good
110 performance for studying the formation of atmospheric molecular clusters.^{53,54} Single
111 point energy calculations at DLPNO-CCSD(T) (Domain-based local pair natural orbital
112 coupled cluster^{55,56})/aug-cc-pVTZ level have been performed in ORCA version 3.0.3.⁵⁷
113 Recent studies indicated that the DLPNO-CCSD(T) method can be used to calculate
114 atmospheric acid-base clusters up to 10 molecules⁵⁸ and the utilized DLPNO-
115 CCSD(T)/aug-cc-pVTZ method has been shown to yield a mean absolute error of 0.3
116 kcal/mol compared to CCSD(T) complete basis set estimates, based on a test set of 11
117 small atmospheric cluster reactions⁵⁴. The MEA monomer has 13 conformations^{6,59} and
118 each was used as a starting point for forming the molecular clusters. For the global
119 minimum search, more than 10000 randomly oriented configurations were built for
120 each cluster. We have estimated the Gibbs free energies for all obtained global minima
121 at 298.15 K by combining the single point energies at the DLPNO-CCSD(T)/aug-cc-
122 pVTZ level and Gibbs free energy correction terms at the ω B97X-D/6-31++G(d,p)
123 level. The formation free energies for each cluster were obtained by subtracting Gibbs
124 free energy of the constituent molecules from that of the cluster at 298.15 K. The

formation free energies at other temperatures were calculated under the assumption that enthalpy and entropy change remain constant in the tropospheric temperature range.

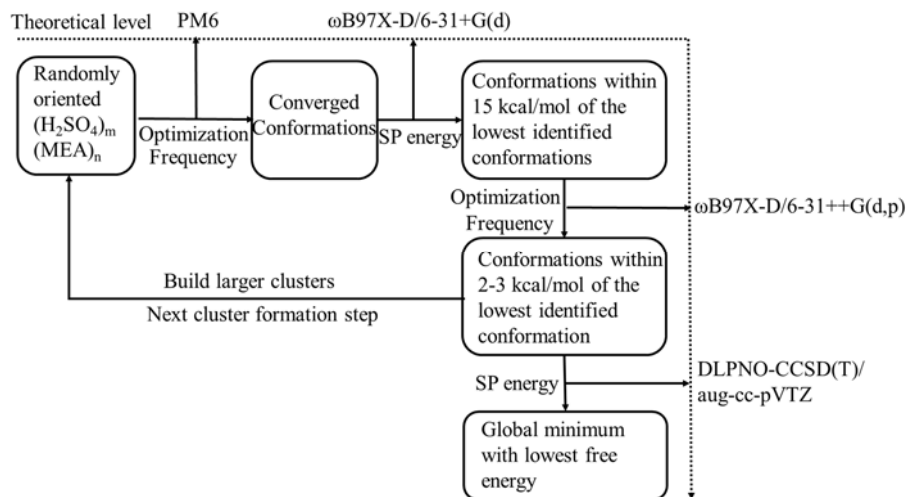


Figure 1. Flowchart for the multistep global minimum sampling method. “SP” represents a single point energy calculation.

To consider the effect of hydration, the $(\text{MEA})_m(\text{SA})_n\text{W}_x$ ($m=0-2$, $n=0-2$, $x=1-3$, “W” represents H_2O) clusters were investigated. For their global minimum search, a similar scheme as for the clusters without water molecules was used. In addition, to directly compare the enhancing effect of MEA to ammonia, MA and DMA, we re-evaluated their formation free energies at the same theoretical level, based on reported cluster structures, or new lower energy structures (presented in Figure S1).^{48, 49, 60} It should be noted that for global minimum of the unhydrated MA-SA clusters, only $(\text{MA})_{0-3}(\text{SA})_{0-3}$ is available^{41,60} and therefore formation free energy data for MA are only for $(\text{MA})_{0-3}(\text{SA})_{0-3}$.

ACDC model. We used ACDC to study the formation pathways, steady-state concentrations and formation rates of clusters. The detailed theory behind the ACDC

141 was present in a study by McGrath et. al.⁴⁷ Briefly, the code generates equations for the
142 time derivatives of the concentrations of all studied clusters, and uses the Matlab ode15s
143 routine to solve differential equations and simulate the time-dependent cluster
144 concentrations. The differential equations, also called birth-death equations, include
145 source terms from collisions of smaller clusters and evaporations from larger clusters,
146 and sink terms from collisions with other clusters and evaporations into smaller clusters.
147 In addition, the cluster formation rate in ACDC is defined as the flux of clusters outside
148 the system. Whether a cluster is allowed to be outside the system or not is judged by
149 the boundary condition. The hydration effect was considered in ACDC by taking H₂O
150 molecule as an environment to affect the collision or evaporation of base-acid cluster.⁶¹
151 The simulated system is a “4 × 4 box” for unhydrated system, where 4 is the maximum
152 number of H₂SO₄ or MEA molecules in the clusters. The (MEA)₄(SA)₅ and
153 (MEA)₅(SA)₅ were allowed to grow out of the system and all other clusters crossing the
154 box edge are brought back to the simulation box by monomer evaporations (see
155 boundary condition in Supporting Information (SI)). The ACDC simulations were
156 primarily run at 278.15 K, with additional runs performed at 258.15, 268.15, 288.15
157 and 298.15 to study the temperature effect. A constant coagulation sink coefficient of
158 $2.6 \times 10^{-3} \text{ s}^{-1}$ was used as sink term. This value corresponds to typical one observed in
159 boreal forest environments.⁴⁸ The sulfuric acid concentration was set to be 10^5 , 10^6 , 10^7 ,
160 10^8 and 10^9 cm^{-3} , a range relevant to atmospheric NPF.^{25,48,62} Atmospheric MEA
161 concentrations were set to be 1, 10, and 100 ppt, a range relevant to atmospheric NPF

for DMA.²⁵ It should be mentioned that the acid concentration $[\text{H}_2\text{SO}_4]$ was defined as the total concentration of all neutral clusters containing one acid and any number of base molecules, as in a previous study.⁴⁸ When hydration effect was considered, the simulated system is “ 2×2 box”. Average collision and evaporation coefficients over the hydrate distribution for each cluster of $(\text{MEA})_m(\text{SA})_n$ ($m=0-2$, $n=0-2$) were used in the birth-death equations for $[\text{H}_2\text{SO}_4] = 10^6$ and $[\text{MEA}] = 10$ ppt and at 278.15 K. The equilibrium hydrate distribution for each cluster was calculated by the equilibrium constant for the formation of the respective hydrate.⁶¹ Similar to the definition of boundary condition of unhydrated MEA-SA cluster, the $(\text{MEA})_2(\text{SA})_3$ and $(\text{MEA})_3(\text{SA})_3$ were allowed to grow out of the system. As a comparison, we also performed ACDC simulation for MA- H_2SO_4 and DMA- H_2SO_4 systems at 278.15 K. The simulated system is a “ 3×3 box” for MA since only $(\text{MA})_{0-3}(\text{SA})_{0-3}$ is available, and “ 4×4 box,” for DMA. The $(\text{MA})_3(\text{SA})_4$ and $(\text{MA})_4(\text{SA})_4$, and $(\text{DMA})_4(\text{SA})_5$ and $(\text{DMA})_5(\text{SA})_5$ were allowed to grow out of the simulation box for MA- H_2SO_4 and DMA- H_2SO_4 system (see SI), respectively. Other ACDC simulation details are similar to those for MEA. In addition, ACDC simulation was performed for MEA- H_2SO_4 with 3×3 box, to compare with MA- H_2SO_4 system with a similar simulation box size.

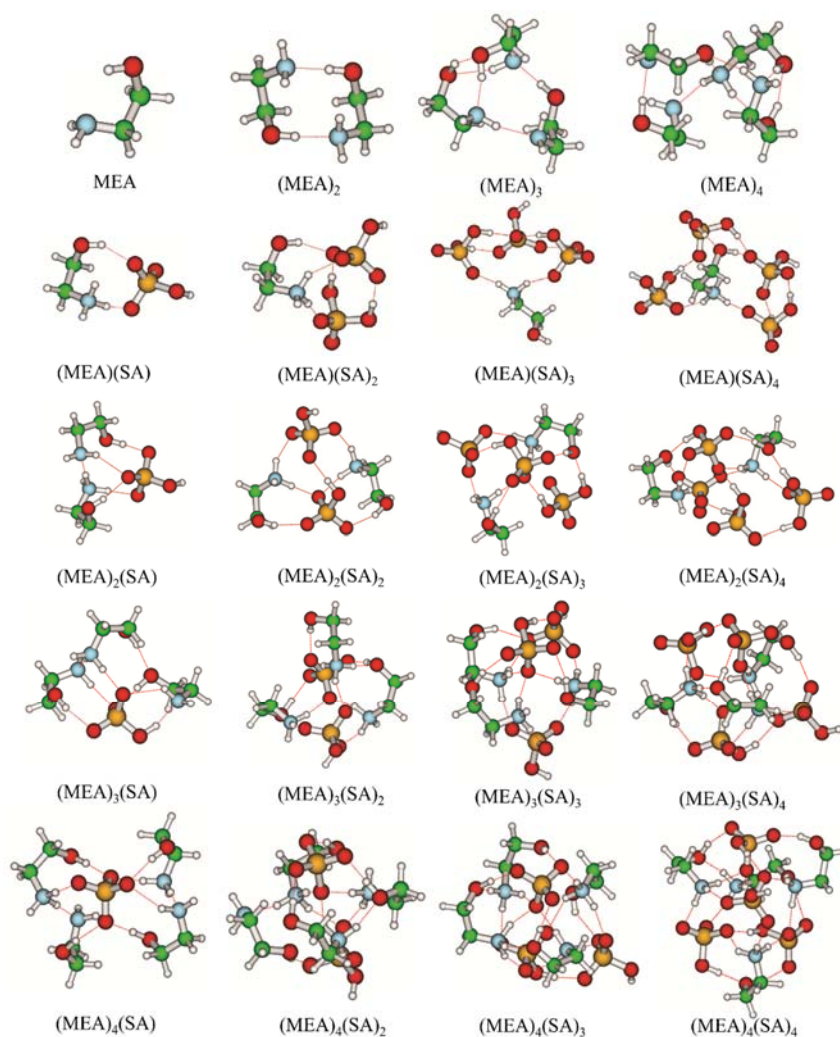
RESULTS AND DISCUSSION

Structures and Thermodynamic Data. We use $(\text{MEA})_m(\text{SA})_n$ to represent the cluster formed by m MEA molecules and n H_2SO_4 molecules to avoid explicitly specifying the proton transfer status. Since previous studies have discussed the structures of pure

183 H₂SO₄ clusters,⁴⁹ here, we mainly focus on the clusters (MEA)_m(SA)_n($m=1-4$ and $n=0-$
 184 4). The structures of (MEA)_m(SA)_n($m=1-4$ and $n=0-4$) are shown in Figure 2. Generally,
 185 in the homo-molecular clusters (MEA)_m($m=1-4$), no proton transfer has occurred and
 186 clusters are stabilized mainly by H-bonds. In all hetero-molecular clusters, proton
 187 transfer is observed, and clusters are stabilized by both H-bonds and electrostatic
 188 interaction between positive and negative species. When $n \geq m$, the amine (-NH₂)
 189 groups of all MEA molecules are protonated by H₂SO₄. In this case H₂SO₄ only
 190 transfers a single proton and in no cases a sulphate ion is formed. When $n < m$, there
 191 are two different proton transfer pattern. For (MEA)₂(SA), (MEA)₃(SA) clusters, none
 192 or one of the protons of H₂SO₄ are donated, and therefore not all MEA molecules are
 193 protonated. For (MEA)₄(SA), (MEA)₄(SA)₂, (MEA)₄(SA)₃ and (MEA)₃(SA)₂, H₂SO₄
 194 can donate two protons, and therefore all MEAs are protonated in the case of $m - n = 1$
 195 ((MEA)₄(SA)₃ and (MEA)₃(SA)₂), while MEA is not completely protonated in the case
 196 of $m - n > 1$ ((MEA)₄(SA) and (MEA)₄(SA)₂). The above proton transfer patterns for
 197 H₂SO₄-MEA clusters are similar to those of H₂SO₄-DMA clusters.^{48,49}

198 Another structural feature in all clusters except (MEA)(SA)₃ is that -OH
 199 groups of all MEAs can form at least one H-bond with H₂SO₄ as H-bond donors. In
 200 many cases such as (MEA)₃, (MEA)₄, (MEA)(SA)₄, (MEA)₂(SA)₃, (MEA)₂(SA)₄,
 201 (MEA)₃(SA)₁, (MEA)₃(SA)₂, (MEA)₃(SA)₄, (MEA)₃(SA)₂, (MEA)₄(SA)₂ and
 202 (MEA)₄(SA)₃ clusters, the -OH group of MEA can form another H-bond with the -OH
 203 group of H₂SO₄, ammonium cation (-RNH₃⁺) of protonated MEA or -OH of MEA as a

204 H-bond acceptor. The involvement of the -OH group of MEA leads to a preference for
 205 a spherical three-dimensional structure, especially for the large studied cluster sizes. As
 206 an exception (MEA)(SA)₃, we also located a low-energy minimum (Figure S2)
 207 involving H-bonds where -OH group of MEA acts as both a hydrogen bond donor and
 208 acceptor. However, the configuration is not the global minimum for the Gibbs free
 209 energy. The binding energy of this minimum is about 1 kcal/mol lower than that of the
 210 free energy global minimum shown in Figure 2, and thus unfavorable entropy effects
 211 are taking place in this configuration.



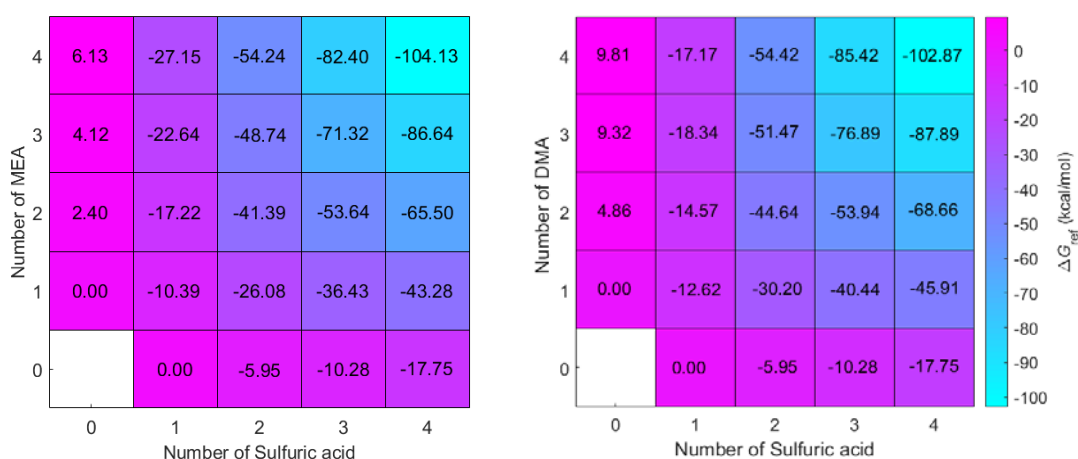
212

213 Figure 2. The Structures of global free energy minima for (MEA)_m(H₂SO₄)_n ($m=1-4$ and

$n=0-4$) at the ω B97X-D/6-31++G(d,p) level of theory. The red ball represents oxygen atom, blue is nitrogen atom, green is carbon atom and white is hydrogen atom.

It is known that DMA is one of the strongest agents for enhancing atmospheric H_2SO_4 -based NPF.^{25,29,43} Here, we take formation free energies of the H_2SO_4 -DMA system as a reference to discuss the formation free energies of H_2SO_4 -MEA. The free energy data at 298.15 K for the formation of the clusters from their constituent molecules for the MEA/DMA- H_2SO_4 system are presented in Figure 3, and the corresponding thermodynamical quantities ΔH and ΔS are presented in Table S1. For the pure base clusters, formation free energy of all MEA clusters is lower than that of corresponding DMA clusters. This results from the fact that there is one more H-bond bonding agent (-OH) in MEA compared with DMA, which leads to more H-bonds in the pure MEA clusters than that in the corresponding DMA clusters. The formation free energy for most hetero-molecular H_2SO_4 -MEA clusters is 0.2-5.6 kcal/mol higher than that of corresponding H_2SO_4 -DMA clusters. However, the formation free energy for $(\text{MEA})_2\text{SA}$, $(\text{MEA})_3\text{SA}$ and $(\text{MEA})_4\text{SA}$ and $(\text{MEA})_4(\text{SA})_4$ is lower than that of the corresponding clusters from DMA. The difference in formation free energies of MEA clusters, compared with DMA clusters, originates from the competition between the unfavorable (lower basicity of MEA than that of DMA) and favorable factor (the formation of more H-bonds from the -OH group of MEA) for forming clusters. In addition, we noted that formation free energies of MEA- H_2SO_4 clusters are lower than those of the corresponding MA- H_2SO_4 clusters (Figure S3) although basicity of MEA

235 is much lower than that of MA, indicating that the -OH group in MEA does indeed play
 236 an important role in the cluster formation between MEA and H₂SO₄. In recent study,
 237 Chen et al. revealed that besides the basicity, the hydrogen-bonding capacity of -NH_x
 238 ($x = 1-3$) group in amine/ammonia can play an important role in enhancing
 239 methanesulfonic acid driven NPF.⁶³ Our findings and Chen et al.'s study⁶³ together
 240 show the importance of molecular interactions involving -NH_x ($x = 1-3$) group and other
 241 functional groups of amines in NPF. In addition, similar to MA and DMA, the
 242 formation free energies for MEA are much lower than those of NH₃ (Figure S3) with
 243 H₂SO₄.



244 Figure 3. Calculated formation free energies for (MEA)_m(SA)_n (left panel) and
 245 (DMA)_m(SA)_n (right panel) clusters ($m=0-4$ and $n=0-4$) at the DLPNO-CCSD(T)/aug-
 246 cc-pVTZ// ω B97X-D/6-31++G(d,p) level and 298.15 K and 1 atm (reference pressure
 247 of acid and base).

248 **Evaporation Rates.** In view of the acid-base cluster growth, the stability of the cluster
 249 can be deduced by comparing the evaporation rate with the collision rate, which mainly
 250 depends on the collision rate constant and the concentration of the acid and base

251 molecules. However, the collision rate constants for the studied clusters are very close
252 to each other and thus difference in the evaporation rate can be used to represent the
253 stability of clusters at the given acid and base concentration. The evaporation rates for
254 $(\text{MEA})_m(\text{SA})_n$ ($m=0-4$ and $n=0-4$) on the MEA-SA grid at 278.15 are presented in Figure
255 4. Generally, evaporation rates for clusters $(\text{MEA})_2(\text{SA})_2$, $(\text{MEA})_1(\text{SA})_2$, $(\text{MEA})_3(\text{SA})_3$,
256 $(\text{MEA})_3(\text{SA})_4$ and $(\text{MEA})_4(\text{SA})_4$ are of the order of 10^{-3} - 10^{-5} s^{-1} , which is much lower
257 than those for other studied cluster sizes. When the concentration of MEA or H_2SO_4 is
258 around or above ppt level, those clusters with evaporation rate 10^{-3} - 10^{-5} s^{-1} can be
259 considered to be stable and $(\text{MEA})_3(\text{SA})_3$ and $(\text{MEA})_4(\text{SA})_4$ are the most stable clusters
260 (see discussion on stability of clusters in SI). By checking all evaporation pathways
261 (see Table S2), evaporation of a H_2SO_4 or MEA monomer is found to be the main decay
262 route for all clusters studied here. If m and n are unequal, evaporation of species with
263 greater number of molecules is always preferred. For clusters with $m = n > 2$,
264 evaporation of MEA is faster than that of H_2SO_4 . In addition, when there is equal
265 number of molecules in two clusters, the evaporation rate of MEA abundant cluster is
266 higher than corresponding H_2SO_4 abundant cluster, indicating that the bonding ability
267 of H_2SO_4 to the cluster is stronger than that of MEA. A similar phenomena concerning
268 the stronger bonding ability of acid is also found in other acid-base cluster systems,
269 such as DMA-SA, NH_3 - H_2SO_4 , and NH_3 - HNO_3 .^{49,64}

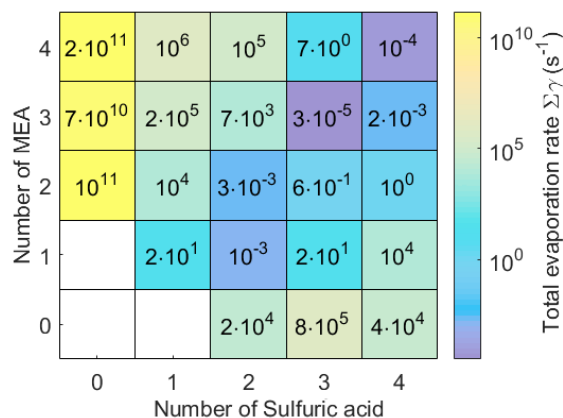


Figure 4. The evaporation rates for $(\text{MEA})_m(\text{SA})_n$ ($m=0-4$ and $n=0-4$) on the MEA-SA grid at 278.15.

It is also interesting to compare cluster evaporate rates for the different amines (MA, DMA and MEA) at the same simulation condition. For most of the clusters, including hetero-molecular and pure base clusters, the evaporation rates for MEA clusters are lower than corresponding ones for MA (Figure S4) and DMA (Figure S4) clusters. However, it is not straightforward to conclude which amine can form the most stable clusters as evaporation rates for a couple of clusters with MA and DMA are lower than those of MEA clusters. If the initially formed one SA and one base cluster (which are crucial for cluster growth at relevant H_2SO_4 and base concentration for MEA, MA and DMA as discussed in the Growth Pathways section) are compared, evaporate rate of $(\text{MEA})(\text{SA})$ is lower than that of $(\text{MA})(\text{SA})$ and higher than that of $(\text{DMA})(\text{SA})$. Therefore, the stability of initially formed clusters for the three types of amine- H_2SO_4 clusters follows the trend $(\text{DMA})(\text{SA}) > (\text{MEA})(\text{SA}) > (\text{MA})(\text{SA})$ at the given acid and base concentrations. In addition, in accordance with a previous study,⁴⁷ the evaporation of small clusters is found to be the main decay route for some of DMA- H_2SO_4 clusters.

This is not the case for MEA-SA and MA-SA clusters, where monomer evaporation is dominant. This results from the higher stability of the small DMA-H₂SO₄ clusters.

Steady-state Cluster Concentrations and Formation Rates. The steady-state sulfuric acid dimer concentration (all clusters including sulfuric acid dimer) and the formation rate of clusters growing out of the simulation box can be taken as two important quantities characterizing the stabilization potential of a given base in H₂SO₄-based NPF.^{25,43,60} Figure 5 shows the steady-state sulfuric acid dimer concentration and the cluster formation rate as a function of monomer concentration (H₂SO₄ concentration in the range 10⁵ - 10⁹ cm⁻³, MEA mixing ratios of 1-100 ppt) at 278.15 K for MEA-H₂SO₄ clusters, along with DMA-H₂SO₄ and MA-H₂SO₄ clusters as a comparison. Generally, the sulfuric acid dimer concentration and the cluster formation rate increase with increasing the concentrations of MEA and H₂SO₄ at the considered condition. The MEA concentration dependence of the sulfuric acid dimer concentration and the cluster formation rate weakens with increasing H₂SO₄ concentration, indicating that the system gradually approaches saturation with respect to MEA at a high H₂SO₄ concentration. Similar behavior is also found in the simulations with MA and DMA as base. More importantly, MEA yields roughly 10–10²-fold dimer concentration and 10²–10³-fold formation rate compared to the simulations with MA as a base, and 0.02-0.2-fold dimer concentration and 0.02–1-fold formation rate as compared to the simulations with DMA as a base, indicating the order of the stabilization potential of these three amines follows: DMA > MEA > MA. It deserves mentioning that MEA-H₂SO₄ formation rates

compared to MA-H₂SO₄ become even higher if the same simulation box size is used for MEA and MA (3×3) (formation rate of MEA-H₂SO₄ will increase 1.1-6 times, compared with 4×4 box). However, the difference in sulfuric acid dimer concentration was similar with different simulation box sizes. As experimental evidence has shown that DMA and MA have an enhancing effect on H₂SO₄-based NPF at ppt level,^{25,43} it can be expected that MEA will have a similar effect with magnitude in between DMA and MA. Therefore, we can conclude that MEA can enhance NPF of H₂SO₄ when the atmospheric concentration of MEA reaches ppt level. The higher stabilization potential of MEA, compared with MA, further verifies the important role of the -OH group of MEA in enhancing NPF involving H₂SO₄, as the basicity of MEA is lower than that of MA. In addition, both the sulfuric acid dimer concentration and the formation rate present negative temperature dependence in the range of 260-300 K, relevant to tropospheric conditions as shown in Figure S5. The negative temperature dependence effect is more prominent at lower MEA (1 ppt) and lower H₂SO₄ concentrations (10^6 cm⁻³).

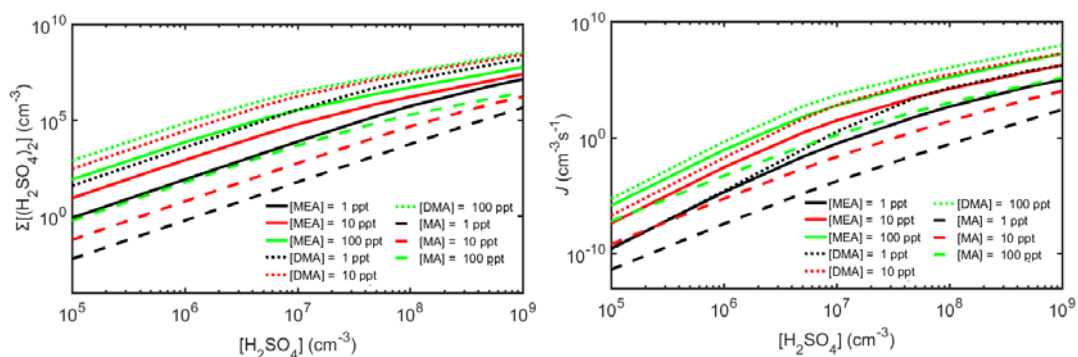


Figure 5. Simulated steady-state H₂SO₄ dimer concentration $\Sigma[(\text{H}_2\text{SO}_4)_2]$ (cm⁻³) (left panel) and the cluster formation rate J (cm³s⁻¹) out of the simulation system (right

panel) as a function of monomer concentration at 278.15 K.

Growth Pathways. Figure 6 presents the growth pathway and the actual Gibbs free energy surface⁴⁷ for MEA and H₂SO₄ clusters at [H₂SO₄] = 10⁶ cm⁻³, [MEA] = 10 ppt and 278.15 K. The actual Gibbs free energy surface was obtained by converting the change of free energy from 1 atm to the actual vapor pressures of the components.⁴⁷ As can be seen in Figure 6 (left panel), the first step in the growth is the binding of one H₂SO₄ molecule to a MEA molecule. After the initial step, the growth mainly proceeds by firstly adding one H₂SO₄, and then one MEA. The main flux out of the system is the (MEA)₄(SA)₅ cluster. Combining the growth pathway with the actual Gibbs free energy surface (right panel in Figure 6), two features can be observed. First, clusters do not follow the lowest free energy pathways ((MEA)₁(SA)₁ → (MEA)₂(SA)₂ → (MEA)₃(SA)₃ → (MEA)₄(SA)₄), which would involve the cluster collision with (MEA)₁(SA)₁ cluster. This results from fact that the concentration of the (MEA)₁(SA)₁ cluster (5.73×10^3 cm⁻³) is much lower than that of the H₂SO₄ monomer (9.94×10^5 cm⁻³). Secondly, the addition of H₂SO₄ monomers involves a small free energy barrier, but the addition of MEA does not. Furthermore, combining the growth pathway with the evaporation rate of the clusters, we can conclude that the formation of initial cluster (MEA)₁(SA)₁ is the rate-determining step for the cluster growth since the (MEA)₁(SA)₁ cluster is much more unstable than other clusters in the cluster growth pathway and readily evaporates back into MEA and SA monomers.

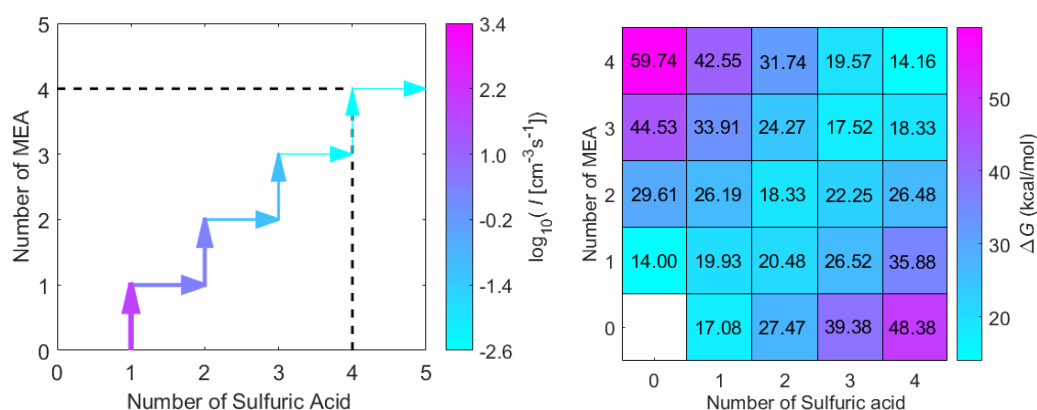


Figure 6. Main clustering pathways (left panel) and actual Gibbs free energy surface for the formation of clusters $\text{MEA}_m(\text{H}_2\text{SO}_4)_n$ ($m=0-4$ and $n=0-4$) (right panel) at 278.15 K, $[\text{H}_2\text{SO}_4] = 10^6 \text{ cm}^{-3}$ and $[\text{MEA}] = 10 \text{ ppt}$. For figure clarity, the pathways contributing less than 5% to the flux of the cluster are not shown.

We also compared the growth pathways for $\text{MEA-H}_2\text{SO}_4$ with $\text{MA-H}_2\text{SO}_4$ and $\text{DMA-H}_2\text{SO}_4$ system at the same simulation condition. The formation pathways for $\text{MA-H}_2\text{SO}_4$ and $\text{DMA-H}_2\text{SO}_4$ are presented in Figure S6. A common feature is that the initially formed cluster mainly consists of one H_2SO_4 and one base molecule for all three amines. However, as a whole, the growth pathway for the $\text{MEA-H}_2\text{SO}_4$ system is significantly different from that of the $\text{MA-H}_2\text{SO}_4$ and $\text{DMA-H}_2\text{SO}_4$ systems. In accordance with a previous study,⁴⁷ collisions involving the $(\text{DMA})_1(\text{SA})_1$ cluster contribute significantly to the growth for DMA-SA system, which makes the growth occur mainly along the diagonal on the acid-base grid. In contrast to MEA and DMA , the cluster growth for the MA system does not follow the diagonal direction and the formation of larger clusters $(\text{MA})_1(\text{SA})_2$ and $(\text{MA})_2(\text{SA})_3$ has two pathways either via

addition of H₂SO₄ or MA. The sulfuric acid dimer has a significant population in the initial clusters, which results from the low stability of the (MA)₁(SA)₂ cluster.

Effect of Hydration. As water is many orders of magnitude more abundant than sulfuric acid and bases in the atmosphere, hydration might change the cluster formation free energies and therefore cluster formation kinetics^{61,65,66} Previous studies have found that clusters consisting of H₂SO₄ and DMA or ammonia are mainly hydrated by less than three H₂O molecules.^{30,61} We expected that MEA-H₂SO₄ clusters could still be hydrated by less than three H₂O molecules although the structure of MEA is different from DMA and ammonia. Here, 1-3 H₂O molecules were considered to study the effect of hydration on the formation kinetics of MEA-H₂SO₄ clusters. In addition, to save computational resources, we only selected the smallest clusters (MEA)_m(SA)_n ($m = 0-2$, $n = 0-2$) as test system to investigate the hydration. Based on the calculated equilibrium hydrate distribution of the clusters at relative humidities (RH) 20%, 50% and 100%, at 278.15 K, converted from calculated Gibbs free energies of stepwise hydration at 278.15 K and 1 atm, we can conclude that sulfuric acid-MEA clusters are only mildly hydrated (0-2 H₂O molecules depending on RH). Details for the discussion on calculated Gibbs free energies of stepwise hydration, optimized structures and the hydrate distribution of the clusters are presented in SI. Here, we mainly focus on the effect of hydration on the cluster formation kinetics.

In principle, hydration can affect the cluster formation rate both through the collision and evaporation rates. However, hydration was found to have little effect on

the collision rate since the collision diameter, an important factor in collision rate coefficients in kinetic collision theory employed in ACDC, changes very little with hydration.⁶¹ Hence, only the effect of hydration on the evaporation rates and formation rates will be discussed in detail. Figure 7 presents the evaporation rates (left) and formation rates (right) as a function of RH at 278.15 K compared to dry conditions. Clearly, the presence of water has various effects on the evaporation rate depending on the given cluster. Water has a little effect on the evaporation rate of the (SA)₂ and (MEA)₂(SA)₂ and almost no effect on that of the (MEA)₂ cluster. However, the evaporation rate of (MEA)(SA)₂ can be increased up to 3 times by hydration, and that of (MEA)₂(SA) can be decreased by 13 times compared to the dry case. More importantly, the presence of water decreases the evaporation rate of initially formed (MEA)(SA) clusters, i.e. the rate-determining step for cluster growth in the system, and this trend gradually increases with RH, which explains the increased cluster formation rate with increasing RH (right panel in Figure 7). The formation rate can be increased about 5 fold at RH = 100 % compared to the dry case. It should be mentioned that although the absolute formation rate obtained from a small simulation box (2×2) is not reliable, the relative formation rate presented here should cancel out any significant bias introduced by the small simulation box. Generally, from these small cluster hydration simulations, we can conclude that hydration can slightly influence the evaporation rate, but the effect is in all cases relatively low and does not severely influence the results. Although it is not expected that qualitative conclusion from current study could be

changed when larger clusters and more water molecules are used, future study with larger clusters and more water molecules is still deserved, to reach a more definitive conclusion about the RH effect on MEA-H₂SO₄ cluster formation kinetics.

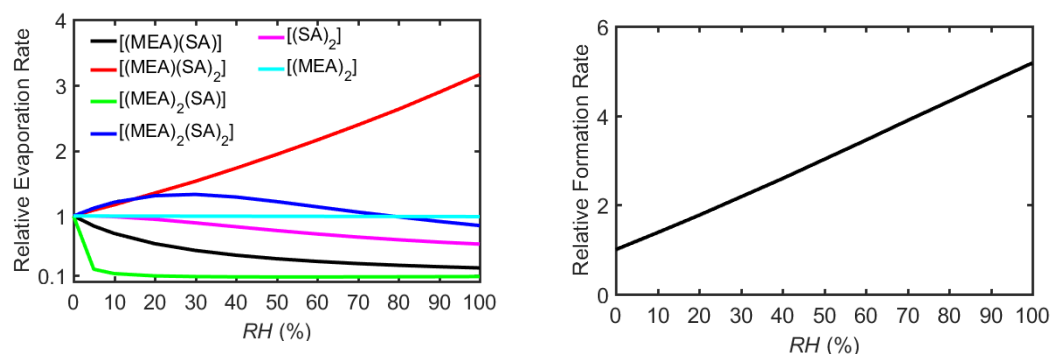


Figure 7. Relative evaporation rate (left panel) and cluster formation rate ($[\text{H}_2\text{SO}_4] = 10^6 \text{ cm}^{-3}$ and $[\text{MEA}] = 10 \text{ ppt}$) (right panel) as a function of relative humidity at 278.15 K.

Atmospheric Implications. We found that MEA at ppt-level can enhance the H₂SO₄-based NPF. The enhancing potential of MEA for NPF is lower than that of DMA, which is one of the strongest agents for enhancing H₂SO₄-based NPF,^{25,43} and much higher than that of MA. In addition, we have shown that the -OH group of MEA plays an important role in enhancing H₂SO₄-based NPF due to the formation of additional H-bonds with H₂SO₄. To the best of our knowledge, this is the first study to point out the significant effect of one additional functional group in amines and show that the basicity of bases is not necessarily the only determining factor influencing H₂SO₄ driven NPF. Besides anthropogenic emission,⁶⁷ the oxidation of aliphatic amines could introduce -OH or keto-, peroxy- and carboxylic acid groups in the atmosphere.^{31,68,69} Amines including these additional H-bond donor/acceptor functional groups can enhance the

NPF via a synergetic role of the basicity and the formation of additional H-bonds, especially for strongly basic amines. As the enhancing effect is very dependent on the exact structure of the molecule, the effect of these amines on NPF deserves further investigation.

Obviously, the participation of MEA in H₂SO₄-based NPF is a sink of the emitted MEA. It is known that the reaction with ·OH is an important sink for MEA due to a high reaction rate constant ($k_{OH} 8.1 \times 10^{-11} \text{ cm}^3 \text{ molecule}^{-1} \text{ s}^{-1}$ at 278.15 K) and concentration of ·OH ($9.7 \times 10^5 \text{ cm}^{-3}$).¹⁸ At daytime, H₂SO₄ and ·OH can coexist in the atmosphere and atmospheric concentration of H₂SO₄ (1×10^6 - $1.9 \times 10^7 \text{ cm}^{-3}$ depending on the location)⁷⁰⁻⁷² is usually 1-19 times that of ·OH. We estimated the relative contribution of H₂SO₄ to ·OH for the removal of MEA by $k_{H_2SO_4}[H_2SO_4]/k_{OH}[\cdot OH]$ at 278.15 K, where $k_{H_2SO_4}$ is removal rate constants of MEA for the participation in NPF involving H₂SO₄ and its value is estimated to be 2.16×10^{-11} and $5.6 \times 10^{-11} \text{ cm}^3 \text{ molecule}^{-1} \text{ s}^{-1}$ at dry or 50% RH condition, respectively (computational details in SI), [H₂SO₄] and [·OH] are the concentration of H₂SO₄ and ·OH, respectively. The contribution of H₂SO₄ to the removal of MEA is calculated to be about 0.27-5.2 and 0.7-13.1 times that of ·OH at dry and 50% RH condition, respectively. This means that reactions with H₂SO₄ will compete with oxidation by ·OH in the atmosphere for the removal of MEA at tropospheric condition. Especially in regions where the concentration of H₂SO₄ is high, NPF might be the dominant removal process of gas-phase MEA. Therefore, the participation of MEA in H₂SO₄-based NPF should be considered when assessing the

environmental risk of MEA emissions related to, for example, postcombustion CO₂ capture technology.

ASSOCIATED CONTENT

Supporting Information. Details for boundary conditions, discussion on the stability of cluster, hydration free energies, removal rate constants of MEA in NPF of H₂SO₄, thermochemical information for the formation of molecular clusters, evaporation coefficients for all evaporation pathways of different clusters, lower energy structures for NH₃-H₂SO₄ and dimethylamine (DMA)-H₂SO₄, low energy structure involving the hydrogen bonds between -OH of all MEA and H₂SO₄, Formation free energies for the clusters for MA/NH₃-H₂SO₄, evaporation rates for MA/DMA-H₂SO₄ clusters, the cluster formation rates and steady-state H₂SO₄ dimer concentrations as a function of temperature, the main clustering pathways for MA/DMA-H₂SO₄ clusters, hydrate distribution of clusters and coordinates of all optimized clusters. This material is available free of charge via the Internet at <http://pubs.acs.org>.

AUTHOR INFORMATION

Corresponding Author

*Phone/fax: +86-411-84707844; e-mail: hbxie@dlut.edu.cn.

ACKNOWLEDGEMENTS

We thank the National Natural Science Foundation of China (21677028, 21325729) and ERC 692891-DAMOCLES. We thank the CSC-IT Center for Science in Espoo, Finland, for computational resources, Jonas Elm thanks the Carlsberg Foundation for financial support and Hong-Bin Xie thanks the China Scholarship Council.

463 **REFERENCES**

- 464 (1) Veawab, A.; Tontiwachwuthikul, P.; Chakma, A., Corrosion Behavior of Carbon
465 Steel in the CO₂ Absorption Process Using Aqueous Amine Solutions. *Ind. Eng. Chem.*
466 *Res.* **1999**, *38* (10), 3917-3924.
- 467 (2) Liu, Y.; Zhang, L.; Watanasiri, S., Representing Vapor–Liquid Equilibrium for an
468 Aqueous MEA-CO₂ System Using the Electrolyte Nonrandom-Two-Liquid Model.
469 *Ind. Eng. Chem. Res.* **1999**, *38* (5), 2080-2090.
- 470 (3) Puxty, G.; Rowland, R.; Allport, A.; Yang, Q.; Bown, M.; Burns, R.; Maeder, M.;
471 Attalla, M., Carbon Dioxide Postcombustion Capture: A Novel Screening Study of
472 the Carbon Dioxide Absorption Performance of 76 Amines. *Environ. Sci. Technol.*
473 **2009**, *43* (16), 6427-6433.
- 474 (4) Xie, H.-B.; He, N.; Song, Z.; Chen, J.; Li, X., Theoretical Investigation on the
475 Different Reaction Mechanisms of Aqueous 2-Amino-2-methyl-1-propanol and
476 Monoethanolamine with CO₂. *Ind. Eng. Chem. Res.* **2014**, *53*, (8), 3363-3372.
- 477 (5) Xie, H.-B.; Johnson, J. K.; Perry, R. J.; Genovese, S.; Wood, B. R., A Computational
478 Study of the Heats of Reaction of Substituted Monoethanolamine with CO₂. *J. Phys.*
479 *Chem. A* **2011**, *115* (3), 342-350.
- 480 (6) Xie, H.-B.; Li, C.; He, N.; Wang, C.; Zhang, S.; Chen, J., Atmospheric Chemical
481 Reactions of Monoethanolamine Initiated by OH Radical: Mechanistic and Kinetic
482 Study. *Environ. Sci. Technol.* **2014**, *48* (3), 1700-1706.
- 483 (7) Xie, H.-B.; Wei, X.; Wang, P.; He, N.; Chen, J., CO₂ Absorption in an Alcoholic
484 Solution of Heavily Hindered Alkanolamine: The Reaction Mechanism of 2-(tert-
485 butylamino)- ethanol with CO₂ Revisited. *J. Phys. Chem. A* **2015**, *119*, 6346-6353
- 486 (8) Xie, H.-B.; Zhou, Y.; Zhang, Y.; Johnson, J. K., Reaction Mechanism of
487 Monoethanolamine with CO₂ in Aqueous Solution from Molecular Modeling. *J. Phys.*
488 *Chem. A* **2010**, *114*, (43), 11844-11852.
- 489 (9) da Silva, E. F.; Booth, A. M., Emissions from Postcombustion CO₂ Capture Plants.
490 *Environ. Sci. Technol.* **2013**, *47* (2), 659-660.
- 491 (10) Kapteina, S.; Slowik, K.; Verevkin, S. P.; Heintz, A., Vapor Pressures and
492 Vaporization Enthalpies of a Series of Ethanolamines. *J. Chem. Eng. Data* **2005**, *50* (2),
493 398-402.
- 494 (11) Karl, M.; Wright, R. F.; Berglen, T. F.; Denby, B., Worst Case Scenario Study to
495 Assess the Environmental Impact of Amine Emissions from a CO₂ Capture Plant. *Int.*
496 *J. Greenhouse Gas Control* **2011**, *5* (3), 439-447.
- 497 (12) Veltman, K.; Singh, B.; Hertwich, E. G., Human and Environmental Impact
498 Assessment of Postcombustion CO₂ Capture Focusing on Emissions from Amine-
499 Based Scrubbing Solvents to Air. *Environ. Sci. Technol.* **2010**, *44* (4), 1496-1502.
- 500 (13) Xie, H.-B.; Ma, F.; Wang, Y.; He, N.; Yu, Q.; Chen, J., Quantum Chemical Study
501 on ·Cl-Initiated Atmospheric Degradation of Monoethanolamine. *Environ. Sci.*
502 *Technol.* **2015**, *49* (22), 13246-13255.
- 503 (14) Karl, M.; Dye, C.; Schmidbauer, N.; Wisthaler, A.; Mikoviny, T.; D'Anna, B.;
504 Müller, M.; Borrás, E.; Clemente, E.; Muñoz, A.; Porras, R.; Ródenas, M.; Vázquez,

505 M.; Brauers, T., Study of OH-initiated Degradation of 2-aminoethanol. *Atmos. Chem.*
506 *Phys.* **2012**, *12* (4), 1881-1901.

507 (15) Karl, M.; Svendby, T.; Walker, S. E.; Velken, A. S.; Castell, N.; Solberg, S.,
508 Modelling atmospheric oxidation of 2-aminoethanol (MEA) emitted from post-
509 combustion capture using WRF–Chem. *Sci. Total Environ.* **2015**, 527–528, 185-202.

510 (16) Nielsen, C. J.; D’Anna, B.; Dye, C.; Graus, M.; Karl, M.; King, S.; Maguto, M.
511 M.; Müller, M.; Schmidbauer, N.; Stenström, Y.; Wisthaler, A.; Pedersen, S.,
512 Atmospheric chemistry of 2-aminoethanol (MEA). *Energy Proc.* **2011**, *4*, 2245-2252.

513 (17) Nielsen, C. J.; Herrmann, H.; Weller, C., Atmospheric Chemistry and
514 Environmental Impact of the Use of Amines in Carbon Capture and Storage (CCS).
515 *Chem. Soc. Rev.* **2012**, *41* (19), 6684-6704.

516 (18) Onel, L.; Blitz, M. A.; Seakins, P. W., Direct Determination of the Rate Coefficient
517 for the Reaction of OH Radicals with Monoethanol Amine (MEA) from 296 to 510 K.
518 *J. Phys. Chem. Lett.* **2012**, *3* (7), 853-856.

519 (19) Borduas, N.; Abbatt, J. P. D.; Murphy, J. G., Gas Phase Oxidation of
520 Monoethanolamine (MEA) with OH Radical and Ozone: Kinetics, Products, and
521 Particles. *Environ. Sci. Technol.* **2013**, *47* (12), 6377-6383.

522 (20) da Silva, G., Atmospheric Chemistry of 2-Aminoethanol (MEA): Reaction of the
523 $\text{NH}_2\text{CHCH}_2\text{OH}$ Radical with O_2 . *J. Phys. Chem. A* **2012**, *116* (45), 10980-10986.

524 (21) Manzoor, S.; Simperler, A.; Korre, A., A Theoretical Study of the Reaction
525 Kinetics of Amines Released into the Atmosphere from CO_2 Capture. *Int. J.*
526 *Greenhouse Gas Control* **2015**, *41*, 219-228.

527 (22) Onel, L.; Blitz, M. A.; Breen, J.; Rickard, A. R.; Seakins, P. W., Branching Ratios
528 for the Reactions of OH with Ethanol Amines Used in Carbon Capture and the Potential
529 Impact on Carcinogen Formation in the Emission Plume from a Carbon Capture Plant.
530 *Phys. Chem. Chem. Phys.* **2015**, *17* (38), 25342-25353.

531 (23) Zhang, R.; Suh, I.; Zhao, J.; Zhang, D.; Fortner, E. C.; Tie, X.; Molina, L. T.;
532 Molina, M. J., Atmospheric New Particle Formation Enhanced by Organic Acids.
533 *Science* **2004**, *304* (5676), 1487-1490.

534 (24) Winkler, P. M.; Steiner, G.; Vrtala, A.; Vehkamäki, H.; Noppel, M.; Lehtinen, K.
535 E. J.; Reischl, G. P.; Wagner, P. E.; Kulmala, M., Heterogeneous Nucleation
536 Experiments Bridging the Scale from Molecular Ion Clusters to Nanoparticles. *Science*
537 **2008**, *319*, (5868), 1374-1377.

538 (25) Almeida, J.; Schobesberger, S.; Kurten, A.; Ortega, I. K.; Kupiainen-Maatta, O.;
539 Praplan, A. P.; Adamov, A.; Amorim, A.; Bianchi, F.; Breitenlechner, M.; David, A.;
540 Dommen, J.; Donahue, N. M.; Downard, A.; Dunne, E.; Duplissy, J.; Ehrhart, S.;
541 Flagan, R. C.; Franchin, A.; Guida, R.; Hakala, J.; Hansel, A.; Heinritzi, M.; Henschel,
542 H.; Jokinen, T.; Junninen, H.; Kajos, M.; Kangasluoma, J.; Keskinen, H.; Kupc, A.;
543 Kurten, T.; Kvashin, A. N.; Laaksonen, A.; Lehtipalo, K.; Leiminger, M.; Leppa, J.;
544 Loukonen, V.; Makhmutov, V.; Mathot, S.; McGrath, M. J.; Nieminen, T.; Olenius, T.;
545 Onnela, A.; Petaja, T.; Riccobono, F.; Riipinen, I.; Rissanen, M.; Rondo, L.;
546 Ruuskanen, T.; Santos, F. D.; Sarnela, N.; Schallhart, S.; Schnitzhofer, R.; Seinfeld, J.

547 H.; Simon, M.; Sipila, M.; Stozhkov, Y.; Stratmann, F.; Tome, A.; Trostl, J.;
 548 Tsagkogeorgas, G.; Vaattovaara, P.; Viisanen, Y.; Virtanen, A.; Vrtala, A.; Wagner, P.
 549 E.; Weingartner, E.; Wex, H.; Williamson, C.; Wimmer, D.; Ye, P.; Yli-Juuti, T.;
 550 Carslaw, K. S.; Kulmala, M.; Curtius, J.; Baltensperger, U.; Worsnop, D. R.;
 551 Vehkamäki, H.; Kirkby, J., Molecular Understanding of Sulphuric Acid-amine Particle
 552 Nucleation in the Atmosphere. *Nature* **2013**, 502 (7471), 359-363.
 553 (26) Ehn, M.; Thornton, J. A.; Kleist, E.; Sipila, M.; Junninen, H.; Pullinen, I.; Springer,
 554 M.; Rubach, F.; Tillmann, R.; Lee, B.; Lopez-Hilfiker, F.; Andres, S.; Acir, I.-H.;
 555 Rissanen, M.; Jokinen, T.; Schobesberger, S.; Kangasluoma, J.; Kontkanen, J.;
 556 Nieminen, T.; Kurten, T.; Nielsen, L. B.; Jorgensen, S.; Kjaergaard, H. G.; Canagaratna,
 557 M.; Maso, M. D.; Berndt, T.; Petaja, T.; Wahner, A.; Kerminen, V.-M.; Kulmala, M.;
 558 Worsnop, D. R.; Wildt, J.; Mentel, T. F., A Large Source of Low-volatility Secondary
 559 Organic Aerosol. *Nature* **2014**, 506, (7489), 476-479.
 560 (27) Wang, Y. H.; Liu, Z. R.; Zhang, J. K.; Hu, B.; Ji, D. S.; Yu, Y. C.; Wang, Y. S.,
 561 Aerosol Physicochemical Properties and Implications for Visibility During an Intense
 562 Haze Episode During Winter in Beijing. *Atmos. Chem. Phys.* **2015**, 15, (6), 3205-3215.
 563 (28) Kirkby, J.; Curtius, J.; Almeida, J.; Dunne, E.; Duplissy, J.; Ehrhart, S.; Franchin,
 564 A.; Gagne, S.; Ickes, L.; Kurten, A.; Kupc, A.; Metzger, A.; Riccobono, F.; Rondo, L.;
 565 Schobesberger, S.; Tsagkogeorgas, G.; Wimmer, D.; Amorim, A.; Bianchi, F.;
 566 Breitenlechner, M.; David, A.; Dommen, J.; Downard, A.; Ehn, M.; Flagan, R. C.;
 567 Haider, S.; Hansel, A.; Hauser, D.; Jud, W.; Junninen, H.; Kreissl, F.; Kvashin, A.;
 568 Laaksonen, A.; Lehtipalo, K.; Lima, J.; Lovejoy, E. R.; Makhmutov, V.; Mathot, S.;
 569 Mikkilä, J.; Minginette, P.; Mogo, S.; Nieminen, T.; Onnela, A.; Pereira, P.; Petaja, T.;
 570 Schnitzhofer, R.; Seinfeld, J. H.; Sipila, M.; Stozhkov, Y.; Stratmann, F.; Tome, A.;
 571 Vanhanen, J.; Viisanen, Y.; Vrtala, A.; Wagner, P. E.; Walther, H.; Weingartner, E.;
 572 Wex, H.; Winkler, P. M.; Carslaw, K. S.; Worsnop, D. R.; Baltensperger, U.; Kulmala,
 573 M., Role of Sulphuric Acid, Ammonia and Galactic Cosmic Rays in Atmospheric
 574 Aerosol Nucleation. *Nature* **2011**, 476 (7361), 429-433.
 575 (29) Kurtén, T.; Loukonen, V.; Vehkamäki, H.; Kulmala, M., Amines Are Likely to
 576 Enhance Neutral and Ion-induced Sulfuric Acid-water Nucleation in the Atmosphere
 577 more Effectively than Ammonia. *Atmos. Chem. Phys.* **2008**, 8 (14), 4095-4103.
 578 (30) Loukonen, V.; Kurtén, T.; Ortega, I. K.; Vehkamäki, H.; Pádua, A. A. H.; Sellegri,
 579 K.; Kulmala, M., Enhancing Effect of Dimethylamine in Sulfuric Acid Nucleation in
 580 the Presence of Water – a Computational Study. *Atmos. Chem. Phys.* **2010**, 10 (10),
 581 4961-4974.
 582 (31) Murphy, S. M.; Sorooshian, A.; Kroll, J. H.; Ng, N. L.; Chhabra, P.; Tong, C.;
 583 Surratt, J. D.; Knipping, E.; Flagan, R. C.; Seinfeld, J. H., Secondary Aerosol Formation
 584 from Atmospheric Reactions of Aliphatic Amines. *Atmos. Chem. Phys.* **2007**, 7 (9),
 585 2313-2337.
 586 (32) Berndt, T.; Stratmann, F.; Sipilä, M.; Vanhanen, J.; Petäjä, T.; Mikkilä, J.; Grüner,
 587 A.; Spindler, G.; Lee Mauldin III, R.; Curtius, J.; Kulmala, M.; Heintzenberg, J.,
 588 Laboratory Study on New Particle Formation from the Reaction OH + SO₂: Influence

589 of Experimental Conditions, H₂O Vapour, NH₃ and the Amine Tert-butylamine on the
 590 Overall Process. *Atmos. Chem. Phys.* **2010**, *10* (15), 7101-7116.
 591 (33) Smith, J. N.; Barsanti, K. C.; Friedli, H. R.; Ehn, M.; Kulmala, M.; Collins, D. R.;
 592 Scheckman, J. H.; Williams, B. J.; McMurry, P. H., Observations of Aminium Salts in
 593 Atmospheric Nanoparticles and Possible Climatic Implications. *Proc. Natl. Acad. Sci.*
 594 **2010**, *107* (15), 6634-6639.
 595 (34) Zhao, J.; Smith, J. N.; Eisele, F. L.; Chen, M.; Kuang, C.; McMurry, P. H.,
 596 Observation of Neutral Sulfuric Acid-amine Containing Clusters in Laboratory and
 597 Ambient Measurements. *Atmos. Chem. Phys.* **2011**, *11* (21), 10823-10836.
 598 (35) Erupe, M. E.; Viggiano, A. A.; Lee, S. H., The Effect of Trimethylamine on
 599 Atmospheric Nucleation Involving H₂SO₄. *Atmos. Chem. Phys.* **2011**, *11* (10), 4767-
 600 4775.
 601 (36) Lehtipalo, K.; Rondo, L.; Kontkanen, J.; Schobesberger, S.; Jokinen, T.; Sarnela,
 602 N.; Kürten, A.; Ehrhart, S.; Franchin, A.; Nieminen, T.; Riccobono, F.; Sipilä, M.; Yli-
 603 Juuti, T.; Duplissy, J.; Adamov, A.; Ahlm, L.; Almeida, J.; Amorim, A.; Bianchi, F.;
 604 Breitenlechner, M.; Dommen, J.; Downard, A. J.; Dunne, E. M.; Flagan, R. C.; Guida,
 605 R.; Hakala, J.; Hansel, A.; Jud, W.; Kangasluoma, J.; Kerminen, V.-M.; Keskinen, H.;
 606 Kim, J.; Kirkby, J.; Kupc, A.; Kupiainen-Määttä, O.; Laaksonen, A.; Lawler, M. J.;
 607 Leiminger, M.; Mathot, S.; Olenius, T.; Ortega, I. K.; Onnela, A.; Petäjä, T.; Praplan,
 608 A.; Rissanen, M. P.; Ruuskanen, T.; Santos, F. D.; Schallhart, S.; Schnitzhofer, R.;
 609 Simon, M.; Smith, J. N.; Tröstl, J.; Tsagkogeorgas, G.; Tomé, A.; Vaattovaara, P.;
 610 Vehkamäki, H.; Vrtala, A. E.; Wagner, P. E.; Williamson, C.; Wimmer, D.; Winkler,
 611 P. M.; Virtanen, A.; Donahue, N. M.; Carslaw, K. S.; Baltensperger, U.; Riipinen, I.;
 612 Curtius, J.; Worsnop, D. R.; Kulmala, M., The Effect of Acid–base Clustering and Ions
 613 on the Growth of Atmospheric Nano-particles. *Nat. Commun.* **2016**, *7*, 11594.
 614 (37) Chen, M.; Titcombe, M.; Jiang, J.; Jen, C.; Kuang, C.; Fischer, M. L.; Eisele, F.
 615 L.; Siepmann, J. I.; Hanson, D. R.; Zhao, J.; McMurry, P. H., Acid–base Chemical
 616 Reaction Model for Nucleation Rates in the Polluted Atmospheric Boundary Layer.
 617 *Proc. Natl. Acad. Sci.* **2012**, *109* (46), 18713-18718.
 618 (38) Xu, Z.-Z.; Fan, H.-J., Competition Between H₂SO₄–(CH₃)₃N and H₂SO₄–H₂O
 619 Interactions: Theoretical Studies on the Clusters [(CH₃)₃N]·(H₂SO₄)·(H₂O)_{3–7}. *J. Phy.*
 620 *Chem. A* **2015**, *119* (34), 9160-9166.
 621 (39) Lv, S.-S.; Miao, S.-K.; Ma, Y.; Zhang, M.-M.; Wen, Y.; Wang, C.-Y.; Zhu, Y.-P.;
 622 Huang, W., Properties and Atmospheric Implication of Methylamine–Sulfuric Acid–
 623 Water Clusters. *J. Phy. Chem. A* **2015**, *119* (32), 8657-8666.
 624 (40) Nadykto, A.; Yu, F.; Jakovleva, M.; Herb, J.; Xu, Y., Amines in the Earth's
 625 Atmosphere: A Density Functional Theory Study of the Thermochemistry of Pre-
 626 Nucleation Clusters. *Entropy* **2011**, *13* (2), 554-569.
 627 (41) Nadykto, A.; Herb, J.; Yu, F.; Xu, Y.; Nazarenko, E., Estimating the Lower Limit
 628 of the Impact of Amines on Nucleation in the Earth's Atmosphere. *Entropy* **2015**, *17*(5),
 629 2764-2780.

630 (42) Nadykto, A. B.; Herb, J.; Yu, F.; Xu, Y., Enhancement in the Production of
 631 Nucleating Clusters due to Dimethylamine and Large Uncertainties in the
 632 Thermochemistry of Amine-enhanced Nucleation. *Chem. Phys. Lett.* **2014**, *609*, 42-49.
 633 (43) Jen, C. N.; McMurry, P. H.; Hanson, D. R., Stabilization of Sulfuric Acid Dimers
 634 by Ammonia, Methylamine, Dimethylamine, and Trimethylamine. *J. Geophys. Res.*
 635 *Atmos.* **2014**, *119* (12), 7502-7514.
 636 (44) Jen, C. N.; Bachman, R.; Zhao, J.; McMurry, P. H.; Hanson, D. R., Diamine-
 637 sulfuric Acid Reactions Are a Potent Source of New Particle Formation. *Geophys. Res.*
 638 *Lett.* **2016**, *43* (2), 867-873.
 639 (45) Elm, J.; Jen, C. N.; Kurtén, T.; Vehkamäki, H., Strong Hydrogen Bonded
 640 Molecular Interactions between Atmospheric Diamines and Sulfuric Acid. *J. Phy.*
 641 *Chem. A* **2016**, *120* (20), 3693-3700.
 642 (46) Hall, H. K., Correlation of the Base Strengths of Amines1. *J. Am. Chem. Soc.* **1957**,
 643 *79* (20), 5441-5444.
 644 (47) McGrath, M. J.; Olenius, T.; Ortega, I. K.; Loukonen, V.; Paasonen, P.; Kurtén,
 645 T.; Kulmala, M.; Vehkamäki, H., Atmospheric Cluster Dynamics Code: a flexible
 646 method for solution of the birth-death equations. *Atmos. Chem. Phys.* **2012**, *12* (5),
 647 2345-2355.
 648 (48) Olenius T, K.-M. O. I., Kurtén T, Vehkamäki H., Free Energy Barrier in the
 649 Growth of Sulfuric Acid–ammonia and Sulfuric Acid–dimethylamine Clusters. *J.*
 650 *Chem. Phys.* **2013**, *139* (8), 084312.
 651 (49) Ortega, I. K.; Kupiainen, O.; Kurtén, T.; Olenius, T.; Wilkman, O.; McGrath, M.
 652 J.; Loukonen, V.; Vehkamäki, H., From Quantum Chemical Formation Free Energies
 653 to Evaporation Rates. *Atmos. Chem. Phys.* **2012**, *12* (1), 225-235.
 654 (50) Elm, J.; Fard, M.; Bilde, M.; Mikkelsen, K. V., Interaction of Glycine with
 655 Common Atmospheric Nucleation Precursors. *J. Phy. Chem. A* **2013**, *117* (48), 12990-
 656 12997.
 657 (51) Elm, J.; Myllys, N.; Hyttinen, N.; Kurtén, T., Computational Study of the
 658 Clustering of a Cyclohexene Autoxidation Product C₆H₈O₇ with Itself and Sulfuric
 659 Acid. *J. Phy. Chem. A* **2015**, *119* (30), 8414-8421.
 660 (52) Frisch, M. J.; Trucks, G. W.; H.B, S.; Scuseria, G. E.; Robb, M. A.; Cheeseman,
 661 J. R., et.al *Gaussian 09*, 2009
 662 (53) Elm, J.; Bilde, M.; Mikkelsen, K. V., Assessment of Binding Energies of
 663 Atmospherically Relevant Clusters. *Phys. Chem. Chem. Phys.* **2013**, *15* (39), 16442-
 664 16445.
 665 (54) Elm, J.; Kristensen, K., Basis Set Convergence of the Binding Eenergies of
 666 Strongly Hydrogen-bonded Atmospheric Clusters. *Phys. Chem. Chem. Phys.* **2017**, *19*
 667 (2), 1122-1133.
 668 (55) Riplinger, C.; Neese, F., An Efficient and Near Linear Scaling Pair Natural Orbital
 669 Based Local Coupled Cluster Method. *J. Chem. Phys.* **2013**, *138* (3), 034106.

670 (56) Riplinger, C.; Sandhoefer, B.; Hansen, A.; Neese, F., Natural Triple Excitations in
 671 Local Coupled Cluster Calculations with Pair Natural Orbitals. *J. Chem. Phys.* **2013**,
 672 *139* (13), 134101.
 673 (57) Neese, F., The ORCA program system. *Wiley Interdiscip. Rev. Comput. Mol. Sci.*
 674 **2012**, *2* (1), 73-78.
 675 (58) Mylly, N.; Elm, J.; Halonen, R.; Kurtén, T.; Vehkamäki, H., Coupled Cluster
 676 Evaluation of the Stability of Atmospheric Acid–Base Clusters with up to 10
 677 Molecules. *J. Phy. Chem. A* **2016**, *120* (4), 621-630.
 678 (59) Vorobyov, I.; Yappert, M. C.; DuPré, D. B., Hydrogen Bonding in Monomers and
 679 Dimers of 2-Aminoethanol. *J. Phy. Chem. A* **2002**, *106* (4), 668-679.
 680 (60) Tinja Olenius, Roope Halonen, Theo Kurtén, Henning Henschel, Oona Kupiainen-
 681 Määttä, Ismael K. Ortega, Hanna Vehkamäki, and Ilona Riipinen, New Particle
 682 Formation from Sulfuric Acid and Amines: Comparison of Mono-, Di-, and
 683 Trimethylamines. *Submitted to Journal of Geophysical Research: Atmospheres*.
 684 (61) Henschel, H.; Kurtén, T.; Vehkamäki, H., Computational Study on the Effect of
 685 Hydration on New Particle Formation in the Sulfuric Acid/Ammonia and Sulfuric
 686 Acid/Dimethylamine Systems. *J. Phy. Chem. A* **2016**, *120* (11), 1886-1896.
 687 (62) Kerminen, V. M.; Petäjä, T.; Manninen, H. E.; Paasonen, P.; Nieminen, T.; Sipilä,
 688 M.; Junninen, H.; Ehn, M.; Gagné, S.; Laakso, L.; Riipinen, I.; Vehkamäki, H.; Kurten,
 689 T.; Ortega, I. K.; Dal Maso, M.; Brus, D.; Hyvärinen, A.; Lihavainen, H.; Leppä, J.;
 690 Lehtinen, K. E. J.; Mirme, A.; Mirme, S.; Hörrak, U.; Berndt, T.; Stratmann, F.; Birmili,
 691 W.; Wiedensohler, A.; Metzger, A.; Dörmann, J.; Baltensperger, U.; Kiendler-Scharr,
 692 A.; Mentel, T. F.; Wildt, J.; Winkler, P. M.; Wagner, P. E.; Petzold, A.; Minikin, A.;
 693 Plass-Dülmer, C.; Pöschl, U.; Laaksonen, A.; Kulmala, M., Atmospheric Nucleation:
 694 Highlights of the EUCAARI Project and Future Directions. *Atmos. Chem. Phys.* **2010**,
 695 *10* (22), 10829-10848.
 696 Chen, H.; Varner, M. E.; Gerber, R. B.; Finlayson-Pitts, B. J., Reactions of
 697 Methanesulfonic Acid with Amines and Ammonia as a Source of New Particles in Air.
 698 *J. Phys. Chem. B* **2016**, *120*(8), 1526-1536.
 699 (64) Ling, J.; Ding, X.; Li, Z.; Yang, J., First-Principles Study of Molecular Clusters
 700 Formed by Nitric Acid and Ammonia. *J. Phy. Chem. A* **2017**, *121* (3), 661-668.
 701 (65) DePalma, J. W.; Wang, J.; Wexler, A. S.; Johnston, M. V., Growth of Ammonium
 702 Bisulfate Clusters by Adsorption of Oxygenated Organic Molecules. *J. Phy. Chem. A*
 703 **2015**, *119* (45), 11191-11198.
 704 (66) DePalma, J. W.; Doren, D. J.; Johnston, M. V., Formation and Growth of
 705 Molecular Clusters Containing Sulfuric Acid, Water, Ammonia, and Dimethylamine.
 706 *J. Phy. Chem. A* **2014**, *118* (29), 5464-5473.
 707 (67) Ge, X.; Wexler, A. S.; Clegg, S. L., Atmospheric Amines – Part I. A review. *Atmos.*
 708 *Environ.* **2011**, *45* (3), 524-546.
 709 (68) Price, D. J.; Clark, C. H.; Tang, X.; Cocker, D. R.; Purvis-Roberts, K. L.; Silva, P.
 710 J., Proposed Chemical Mechanisms leading to Secondary Organic Aerosol in the

711 Reactions of Aliphatic Amines with Hydroxyl and Nitrate Radicals. *Atmos. Environ.*
712 **2014**, 96, 135-144.

713 (69) Angelino, S.; Suess, D. T.; Prather, K. A., Formation of Aerosol Particles from
714 Reactions of Secondary and Tertiary Alkylamines: Characterization by Aerosol Time-
715 of-Flight Mass Spectrometry. *Environ. Sci. Technol.* **2001**, 35 (15), 3130-3138.

716 (70) Zheng, J.; Hu, M.; Zhang, R.; Yue, D.; Wang, Z.; Guo, S.; Li, X.; Bohn, B.; Shao,
717 M.; He, L.; Huang, X.; Wiedensohler, A.; Zhu, T., Measurements of Gaseous H₂SO₄
718 by AP-ID-CIMS During CAREBeijing 2008 Campaign. *Atmos. Chem. Phys.* **2011**, 11
719 (15), 7755-7765.

720 (71) Berresheim, H.; Elste, T.; Tremmel, H. G.; Allen, A. G.; Hansson, H. C.; Rosman,
721 K.; Dal Maso, M.; Mäkelä, J. M.; Kulmala, M.; O'Dowd, C. D., Gas-aerosol
722 relationships of H₂SO₄, MSA, and OH: Observations in the Coastal Marine Boundary
723 Layer at Mace Head, Ireland. *J. Geophys. Res. Atmos.* **2002**, 107 (D19), PAR 5-1-PAR
724 5-12.

725 (72) Jokinen, T.; Sipilä, M.; Junninen, H.; Ehn, M.; Lönn, G.; Hakala, J.; Petäjä, T.;
726 Mauldin III, R. L.; Kulmala, M.; Worsnop, D. R., Atmospheric Sulphuric Acid and
727 Neutral Cluster Measurements Using CI-API-TOF. *Atmos. Chem. Phys.* **2012**, 12, (9),
728 4117-4125.